# GEOMETRICAL MODELLING OF CORNEAL STRUCTURE IN NON-PATHOLOGICAL INITIAL CONDITIONS. A COMPARATIVE STUDY.

Carmelo Gómez[1], David Piñero[2], José S. Velázquez[3], Francisco L. Sáez-Gutiérrez[1,3], Jorge Alió[4] y Francisco Cavas[3]*

[1] Universidad Politécnica de Cartagena. Escuela Internacional de Doctorado. Calle Fleming, s/n - 32202 Cartagena, Murcia (España).

[2] Universidad de Alicante. Grupo de Optica y Percepción Visual. Carretera San Vicente del Raspeig, s/n - 03690 San Vicente del Raspeig, Alicante (España).

[3] Universidad Politécnica de Cartagena. Dpto de Estructuras, Construcción y Expresión Gráfica. Calle Fleming, s/n - 32202 Cartagena, Murcia (España).

[4] VISSUM. Unidad de Quetarocono. Calle Cabañal, 1 - 03016 Alicante (España)

*ABSTRACT:*

*Modelling and numerical simulation have involved a great advance in clinical practice for the prediction of the structural behaviour of soft tissues in certain healthy or pathological scenarios. One of the main features of these simulations is that they can define the geometric parameters of the structure in its initial boundary conditions. In the case of the cornea, there are discrepancies with respect to the initial conditions that depend on whether if it is considered its physiological geometry measured in vivo, or otherwise its geometry in its stress-free state. The choice of one or the other could lead to errors in the simulation model due to the non-linearity of these tissues. In this study, two methodologies were evaluated, the displacement method and the prestress method, to obtain the geometry of non-pathological cornea in its free-of-stress state. Both methodologies allow obtaining the physiological geometry measured in-vivo of the healthy cornea, however, the method of displacements presents a computational architecture that makes it more efficient in numerical simulation, when compared to the pre-stress method.*

*Keywords: 3D Modelling; Computational Modelling; Ophthalmology; Biological Morphology.*

## 1 Introduction

The human eye is a complex lens system composed of 4 structures through which light must pass until it reaches the retina. Of the four structures, the cornea is the one with the highest optical power, with approximately 40 dioptres, and is characterized because its morphology varies depending on the physiological scenario in which it is located, that is, healthy or pathological [1]. Transparency, optical capabilities, and their gradual structural-slope decline with age are of interest in ophthalmological research [2] due to their important optical refractive properties, because of their high social impact.

One of the main problems for the study of modelling and computational simulation of in-silico corneal biomechanics is the lack of agreement on the physiological geometry of the cornea since different models can be considered to reconstruct the geometry of corneal surfaces [3]. Specifically, from the physiological state of corneal equilibrium, the corneal structure at the macroscopic level can be modelled geometrically using models based on modal or zonal mathematical methods, having been both methods validated to characterize corneal geometry in different clinical scenarios [1].

In these scenarios, the morphology of the corneal hemi-spherical structure is captured in-vivo. This structure is subjected to a tensional balance between intra-corneal (Intra Ocular Pressure or IOP) and extra-corneal (Atmospheric Pressure or AP) forces that make the cornea acquire a stable and defined geometry for each patient in their biological state [4,5]. This geometry is obtained after a process of geometric reconstruction using modal or zonal methods from a discrete and finite set of spatial points obtained after 3D scanning using corneal tomographers [6]. However, geometry in physiological state at the macroscopic level is not the same as corneal geometry in its initial state or in its stress-free state [7-9].

The computational models used to simulate the biomechanical behaviour of the cornea depend on the initial geometry implemented in the in-silico model [10]. There are discrepancies in the scientific literature about considering physiological geometry or a stress-free geometric state for the analysis, mainly motivated by the nonlinear behaviour of the corneal tissue, i.e., whether or not to consider the initial stress-free state could lead to calculation errors in numerical simulation models [11-12].

With respect to Finite Elements Method (FEM) models that consider in the definition of their initial conditions the free stress geometry, this state can be obtained from two methods, the so-called displacement method [11] or the pre-stress method [13,14].

In this research work, two methodologies are designed to determine the stress-free geometry or inverse geometry of the in-vivo state of the non-pathological or healthy cornea, to stablish a comparison between them by considering for the first time the geometry and intraocular pressure specific patient.

## 2 Materials and methods

### 2.1 Participants

This study involved a patient 40 years (male, G0). The inclusion criterion was patient with both healthy eyes and no previous clinical history of eye surgery. The patient signed an informed consent to participate in the clinical study that was carried out according to the ethical standards agreed by the Declaration of Helsinki (7th revision, October 2013, Fortaleza, Brazil). The patient was part of the Iberia Biobank (Universidad Miguel Hernández de Elche, OFTARED-ISCIII). The study was approved by the UPCT ethics committee (CEI21_001).

**Table 1.** Summary of the clinical characteristics of the evaluated healthy patient according to the level of severity of the disease defined using the Amsler-Krumeich classification. Abbreviations: IOP, intraocular pressure (mmHg); Axial Length (mm); Sphere (diopters); Cylinder (diopters); SE, spherical equivalent (diopters); CDVA, corrected distance visual acuity.

| A-K | IOP | 3km_A-K | Eye | Axial Length | Sphere | Cylinder | SE | CDVA |
| --- | --- | --- | --- | --- | --- | --- | --- | --- |
| G0 | 18 | 43.45 | OS | 22.92 | 1.5 | -0.25 | 1.38 | 1 |

### 2.2 Definition of geometry.

The corneal volume is a geometrical entity necessary for FEM analysis and its generation is based on three surfaces: the anterior and posterior surfaces on the one side, and the cornea-sclera intermediate surface on the other side. These three surfaces are generated by zonal methods using B-Splines functions in the Rhinoceros v5.0 software, being obtained from a dense, discrete and finite set or "cloud of data" (raw data) that is generated from the surface scan performed on the cornea by the Sirius tomographer (CSO, Italy). Once the surfaces are defined, the geometric model is generated using SolidWorks v2016 software [1,15,16]. In the scientific literature there are numerous papers that have used these softwares for the modelling of biological structures [1-2].

Regarding the characterization of the material, some studies have shown that the corneal structure is formed by a dense and complex grouping of grade IV collagen fibres in a matrix form, well-structured and perfectly crisscrossed, that give the corneal structure a mechanical singularity [17]. That is why from a numerical simulation point of view, the effect of considering a fibre-reinforced continuum is important, and that is why the vast majority of studies in this field consider anisotropic models for their analysis. In general, it is observed that there is agreement regarding the distribution of collagen fibres in the most important components of the human eye:

- The cornea has two preferential directions: nasal-temporal and inferior-superior
- The limb has a preferential direction: circumferential
- The sclera, for numerical purposes, is considered an isotropic material

Through experimental tests, the mechanical behaviour of any type of material can be characterised, but according to some authors, an experimental study on corneal biomechanics with few tests is a poorly conditioned problem [8,9]. However, some research promoted by other authors presents a sufficient set of data to perform the study of mechanical characterization of the cornea, and for this study we have considered an anisotropic hyper elastic material with incompressible behaviour [10,11].

Publicaciones DYNA SL -- c) Mazarredo nº69 - 2º -- 48009-BILBAO (SPAIN)
Tel +34 944 237 566 – www.revistadyna.com - email: dyna@revistadyna.com
Pag. 2 / 9

## 2.3 Material definition:

It is widely accepted that corneal tissue can be treated as an anisotropic hyperelastic material model. In this research, a standardized exponential material model implemented in ANSYS software (Swanson Analysis System Inc. Canonsburg, PA, USA) was considered.

The strain energy density function ($\psi$) is split into a volumetric and isochoric component where the isochoric component is composed by an isotropic and an anisotropic component to consider the extracellular matrix and collagen fibers contribution respectively (Equations 1-4).

$$\psi = \psi_{volumetric} + \overline{\psi}_{isotropic} + \overline{\psi}_{anisotropic} \text{ (Equation 1)}$$

$$\psi_{volumetric} = \frac{1}{d}(J-1)^2 \text{ (Equation 2)}$$

$$\overline{\psi}_{isotropic} = a_1(\overline{I}_1\text{-3}) + a_2(\overline{I}_2\text{-3}) \text{ (Equation 3)}$$

$$\overline{\psi}_{anisotropic} = \frac{k_1}{2k_2}\left(\exp\left[k_2\left(\overline{I}_4\text{-1}\right)^2\right]\text{-1}\right) + \frac{k_1}{2k_2}\left(\exp\left[k_2\left(\overline{I}_6\text{-1}\right)^2\right]\text{-1}\right) \text{ (Equation 4)}$$

In these equations, $J = det(\mathbf{F})$ considers the volumetric change of the initial volume depending on the deformation tensor $\mathbf{F} = \frac{\partial \mathbf{x}}{\partial \mathbf{X}}$ ($\mathbf{X}$ and $\mathbf{x}$ are the coordinates in the initial and deformed configuration). The deformation tensor is divided in a volumetric and deviatoric deformation expressed as $\mathbf{F} = J^{\frac{1}{3}}\overline{\mathbf{F}}$

The invariants $\overline{I}_1$ , $\overline{I}_2$ , $\overline{I}_4$ and $\overline{I}_6$ are calculated from the modified Right Cauchy Green deformation tensor $\overline{\mathbf{C}} = \overline{\mathbf{F}}^T\overline{\mathbf{F}}$ and structural tensors that consider the preferential fibers orientation $\mathbf{m_0}$ and $\mathbf{n_0}$ according to Equations 5-8)

$$\overline{I}_1 = tr(\overline{\mathbf{C}}) \quad , \quad \overline{I}_2 = \left(\frac{1}{2}\right)\left[\left(tr(\overline{\mathbf{C}})\right)^2 - tr(\overline{\mathbf{C}}^2)\right] \text{ (Equation 5 and 6)}$$

$$\overline{I}_4 = \mathbf{m_0}\overline{\mathbf{C}}\mathbf{m_0} \, , \, \overline{I}_6 = \mathbf{n_0}\overline{\mathbf{C}}\mathbf{n_0} \quad \text{(Equation 7 and 8)}$$

Constant parameters have been obtained from previous works [10,19]. The compressibility factor $d = \frac{2}{K}$ has been evaluated with a bulk factor $K = 5.5$ MPa, $a_1 = 40000 \, Pa$, $a_2 = -10000 \, Pa$, $k_2 = 200$ and $k_1$ has a variable value between 25000 Pa and 50000 Pa to consider zones with different fibers' concentration.

## 2.4 Meshing

To optimize the time needed for calculations, as well as to optimize the goodness of the solution, the right mesh size should be sought. For these types of problems, it has been found that optimal mesh size is based on a minimum of 4 elements in the thickness increasing this number to 6 for dynamic fluid coupling analysis [10]. Finally, the total number of elements is 1024 and of nodes 6138 for the mesh. The type of element used for the analysis has been SOLID186, with three-dimensional elements, composed of 20 nodes and quadratic behaviour. This mesh supports hyper-elasticity, large deformations and large displacements and presents a mixed formulation u-P, useful for incompressible hyper elastic materials. In our studio we used Ansys software for MEF modelling.

## 2.5 Boundary conditions. Displacement method. Pre-stress method

In structural analysis, when a simplification is carried out, usually by removing a component of a system, it is critical that the interaction between the eliminated and remaining elements that previously existed could be reproduced as accurately as possible. Applied to the case of corneal biomechanics, research usually takes two paths: simulating a complete model (sclera and cornea) or a simplified model (cornea) [3]. In our study we have used a simplified corneal model.

Of all the components of the FEM model, the most critical component to achieve model convergence is the number of sub-steps into which the applied load is divided. The accuracy of the results is not significantly affected by the number of steps into which pressure is divided, but there is a number of steps from which the model does not converge. For a geometrical cornea, the value oscillates around 50 sub-steps. In models with large deformations, distributing the application of the load over time is particularly useful, especially when the material models have non-linearities.

With respect to inverse geometry or the stress-free geometric state, two methods exist:

- The displacement method (Figure 1): allows this geometric state to be obtained by an iterative process in which this geometry is assumed, and intraocular pressure is applied. The resulting geometry is compared to the geometry measured with the topographer until the difference between them two is below a certain fixed threshold. This method was initially proposed by A. Pandolfi and G.A. Holzapfel [11] and, subsequently modified by Elsheikh et al. [12].
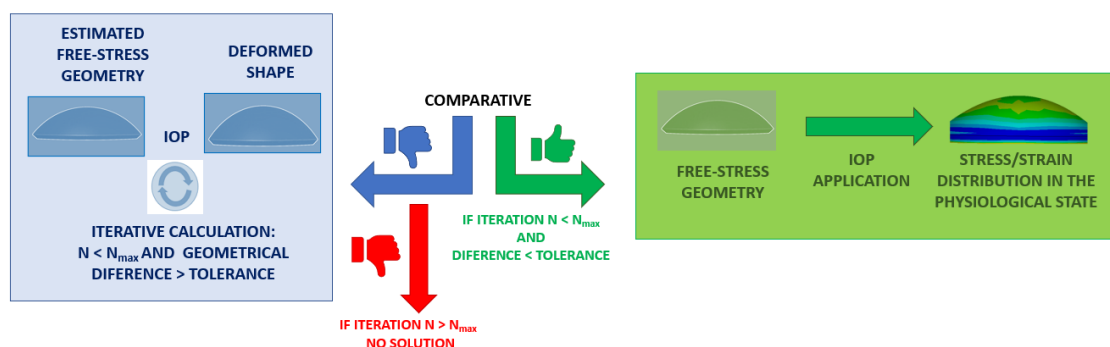


**Fig. 1.** Displacement method (schematic process)

The main characteristic of this methodology is that it can be implemented in any commercial numerical simulation model, since it does not depend on the characteristics of the material, or the type of material considered in the study.

- The pre-stress method (Figure 2). This method is characterized by the fact that it does not allow to directly obtain the free geometry or stress-free state, but it looks for an initial pre-stress state of the tissue that makes deformation almost null when the intraocular pressure is applied, or in other words the field of stress balances the IOP and therefore the resulting geometry practically coincides with the one of the corneal topographer. Computationally it consists of solving the static problem as many times as necessary so that the displacement field is cancelled.

If only this pre-stress is considered as load once it has been calculated, the stress-free geometry can be calculated. This method was presented by Lanchares et al [13,14].
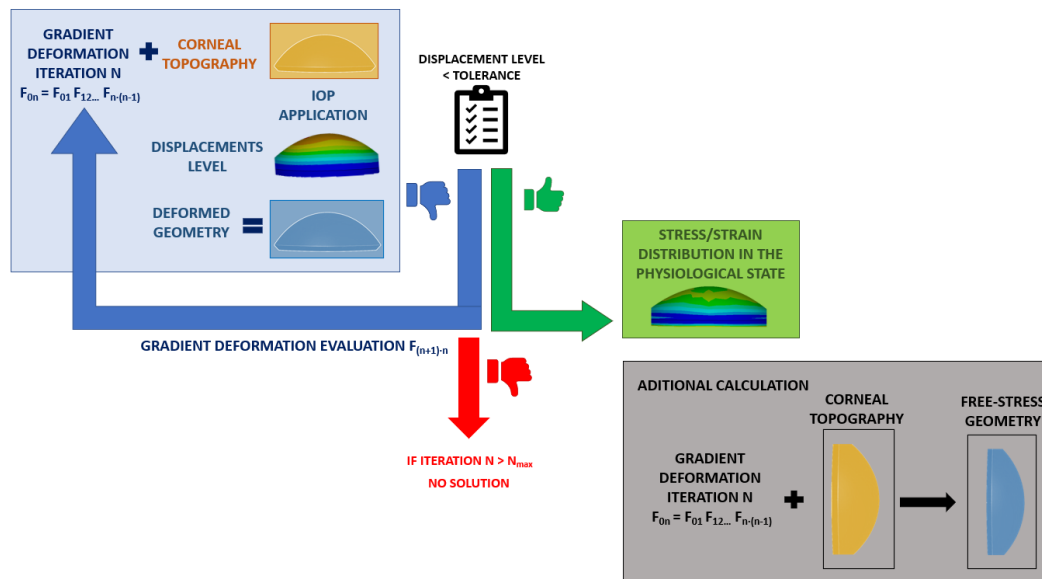
**Fig. 2.** Pre-stress method (schematic process)

## 2.6 Statistics

The statistical analysis of the outcomes obtained was performed using the software SPSS version 15.0 for Windows (SPSS, Chicago, IL). Normality of all data distributions was confirmed by means of the Kolmogorov–Smirnov test. Then, parametric statistics was always applied. Differences between X, Y and Z positions calculated with the displacement and pre-stress methods for the different point evaluated were analysed using the paired Student t test. All statistical tests were two-tailed, and p-values less than 0.05 were considered statistically significant.

## 3 Results

Table 2 summarizes the results of the comparison of the simulations obtained with the two methods of simulation, displacement, and pre-stress, in the healthy cornea. As shown, differences between methods were small in magnitude and did not reach statistical significance, except for the Y and Z position of points on the anterior ($p \leq 0.001$) and posterior corneal surface ($p \leq 0.020$).

**Table 2.** Comparison of the results of the simulations performed in the healthy cornea with the displacement and pre-stress methods.

| Mean (SD) Range | Displacement method | Pre-stress method | P-value |
|---|---|---|---|
| *Anterior corneal surface* | | | |
| **X (mm)** | -0.0081 (3.0641) | -0.0072 (3.0652) | 0.058 |
| | -5.75 to 5.74 | -5.75 to 5.74 | |
| **Y (mm)** | 0.0037 (3.0596) | 0.0019 (3.0591) | 0.001 |
| | -5.74 to 5.75 | -5.74 to 5.75 | |
| **Z (mm)** | 1.4346 (0.8992) | 1.4377 (0.8979) | <0.001 |
| | 0.22 to 2.88 | 0.22 to 2.88 | |
| *Posterior corneal surface* | | | |
| **X (mm)** | -0.0014 (2.7571) | -0.0004 (2.7548) | 0.109 |
| | -5.11 to 5.13 | -5.11 to 5.13 | |
| **Y (mm)** | -0.0011 (2.7547) | -0.0025 (2.7524) | 0.020 |
| | -5.15 to 5.15 | -5.15 to 5.15 | |
| **Z (mm)** | 2.0688 (0.8888) | 2.0712 (0.8868) | <0.001 |
| | 0.85 to 3.41 | 0.85 to 3.41 | |

Publicaciones DYNA SL -- c) Mazarredo nº69 - 2º -- 48009-BILBAO (SPAIN)
Tel +34 944 237 566 – www.revistadyna.com - email: dyna@revistadyna.com

Pag. 5 / 9

Weak but statistically significant correlations of the difference between displacement and pre-stress methods in X ($r = -0.343$, $p = 0.009$) and Z ($r = -0.348$, $p = 0.008$) coordinates on the posterior corneal surface with the distance of location of the point evaluated were found.
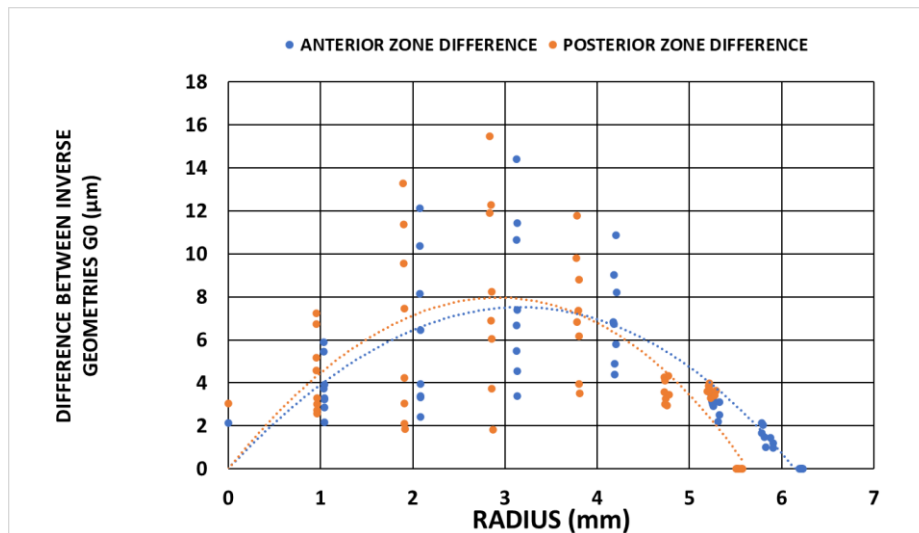


**Fig. 3.** Difference between inverse geometries between displacement and pre-stress methods.

When the inverse geometries obtained by both methods (Figure 3) are compared, it can be observed that the maximum difference between both methods is 14.4 microns for the anterior surface and 15.5 microns for the posterior surface, with an average value of the total difference between the inverse geometries of 4.50 (standard deviation 3.57 microns).
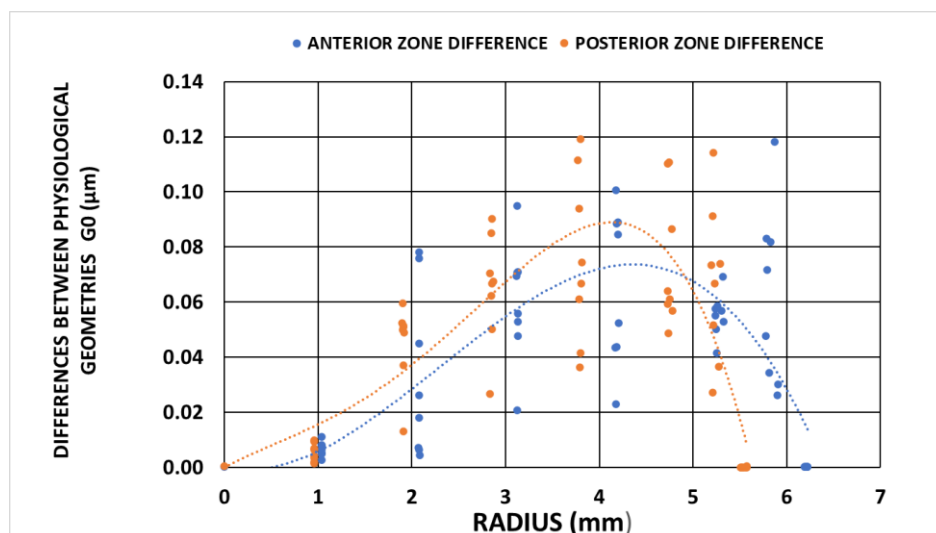


**Fig. 4.** Difference between physiological geometries between displacement and pre-stress methods.

If the physiological or biological geometries obtained by both methods are compared, the results show that the maximum difference between both methods for the anterior surface is $1.18 \cdot 10^{-01}$ microns and is $1.19 \cdot 10^{-01}$ microns for the posterior surface, with a mean value of the total difference between the physiological geometries of 0.04 (standard deviation 0.03 microns) (figure 4).

Publicaciones DYNA SL -- c) Mazarredo nº69 - 2º -- 48009-BILBAO (SPAIN)
Tel +34 944 237 566 – www.revistadyna.com - email: dyna@revistadyna.com

Pag. 6 / 9

## 4 Discussion

Biological structures are not stress-free in their reference configuration but are subject to certain levels of initial residual pretension in physiological load states [20-22]. The mission of these residual stresses depends on the nature of the biological tissue. In the case of arteries, the residual pretensions reduce the internal circumference tension and the tension gradient in the arterial wall [23], and in the case of the ligaments, the pretensions provide stability to the joint in the presence of external loads [24]. With respect to our study, in the case of the cornea the residual stresses serve to maintain the curvature of its greater optical potency in the absence of intracorneal and extracorneal factors [1].

Due to the nonlinearity of these tissues and the exponential character of their behavior curve, the failure to include residual stresses in the computational mechanical models can lead to numerical errors in the calculation of strains.

In fact, physically it can be observed in the cornea that if a longitudinal incision is made according to a random axis, the two parts in which they are divided modify the curvature of their affected surface, which indicates that the residual stresses existing in this corneal region have been released.

It is for this reason that the difficulty of biomechanical modelling of the cornea resides in achieving the correct reproduction of its geometry in the various physiological states that affect the visual capacity of patients. The use of imaging techniques, such as the Scheimpflug camera, allows to visualize the complete geometry of the corneal structure in-vivo and in its physiological state [1]. Several works have applied this technique in order to observe geometric changes in the corneal structure in different pathological scenarios [2,3,18]. However, the application of this technique to geometric modelling when considering the boundary conditions of biomechanical models based on FEM may imply a certain degree of imprecision [2,4], due to the non-linearity and exponential nature of the behavior of corneal tissues. This motivates the appearance in the scientific literature of research works that use two different geometries in the definition of their FEM model, on the one hand there are studies that consider the physiological geometry obtained by Scheimpflug photography [3] and on the other hand there are works that consider the stress-free geometry [7].

To solve the models that consider stress-free geometry there are two methodologies. One method is the so-called pre-stress method [13], which is based on an elastoestatic approach, and consists of reversing the application of intraocular pressure to estimate the stress-free geometric configuration. Another method is the so-called displacement method [11], which is based on a modification of the updated langrian formulation based on the reduction of geometric tolerances, therefore avoids having to calculate in a later process the stress-free geometric configuration.

In this study, the free geometry obtained from both methods has been evaluated. With respect to obtaining the inverse or free-of-stress geometry, there are significant differences with respect to the spatial coordinate Z ($p < 0.001$) for both the anterior surface and the posterior surface, these results coincide with those presented by other authors with respect to the point of maximum curvature Z in healthy patients [15,16,18], and in the central and paracentral region (radius = 0 .. 4 mm) (Figure 3). That is, because in the central and paracentral region the maximum fibrillar distribution density (orthogonal fibers) this shift towards the upper-temporal region, and this decreases its concentration in the transition zone towards the peripheral zone, and in the peripheral area itself (circumferential fibers), the point of maximum curvature Z may vary depending on the fibrillary distribution of each patient.

Conversely, it is observed that when Inverse Geometry is obtained by both methods, there is in fact a significant difference in average value between both methods for such obtained geometry (4.5 ± 3.57 microns), this could be due to the fact that the reverse elastostatic method does not allow the inverse geometry to be obtained directly, but involves an intermediate step, that is to say it requires a complete initial analysis to update the strain gradient tensor to achieve a stress state that balances the OIP, therefore the model starts from a geometry that coincides with the physiological one, but which is subjected to a state of non-zero stresses (Figure 2).

Nonetheless, when each patient's IOP is applied to each model of inverse geometry to obtain the physiological geometry, can be observed that the average value of the total difference between both methods is practically negligible (0.04 ± 0.03 microns), and therefore, both methods work differently when obtaining the reverse geometry, but they are equivalent when obtaining the physiological geometry in healthy corneas (Figures 3-4).

From the point of view of computational behavior, both methods are different since the displacement method allows to obtain the inverse geometry directly (Figure 1) and the pre-stress method does not allow it, needing one more step (Figure 2) to obtain the inverse geometry.

## 5 Conclusion

A characteristic feature of biological tissues such as the cornea, is that under physiological conditions they are subjected to residual stresses caused by the non-linearity and mechanical characteristics of their tissues. Failure to consider the stress-free geometric state

in the definition of the initial conditions of the MEF model, used for biomechanical simulation, could lead to calculation errors in the computational model. In this study two methodologies have been compared to obtain the inverse geometry in healthy corneas, the results obtained show that both methods are very similar, but not equal when it comes to obtaining the inverse geometry, especially from the computational point of view. Nevertheless, both methods could be considered equivalent when obtaining the physiological geometry of the cornea from its inverse geometry applying for each patient its own intraocular pressure.

# References

1. Cavas-Martínez, F.; De la Cruz Sánchez, E.; Nieto Martínez, J.; Fernández Cañavate, F.J.; Fernández-Pacheco, D.G. Corneal topography in keratoconus: state of the art. *Eye and vision (London, England)* **2016**, *3*, 5, doi:10.1186/s40662-016-0036-8.

2. Ma, J.; Wang, Y.; Wei, P.; Jhanji, V. Biomechanics and structure of the cornea: implications and association with corneal disorders. *Survey of ophthalmology* **2018**, *63*, 851-861, doi:10.1016/j.survophthal.2018.05.004.

3. Kling, S.; Hafezi, F. Corneal biomechanics - a review. *Ophthalmic & physiological optics : the journal of the British College of Ophthalmic Opticians (Optometrists)* **2017**, *37*, 240-252, doi:10.1111/opo.12345.

4. Bryant, M.R.; McDonnell, P.J. Constitutive laws for biomechanical modeling of refractive surgery. *Journal of biomechanical engineering* **1996**, *118*, 473-481, doi:10.1115/1.2796033.

5. Buzard, K.A. Introduction to biomechanics of the cornea. *Refractive & corneal surgery* **1992**, *8*, 127-138.

6. Navarro, R.; González, L.; Hernández, J.L. Optics of the average normal cornea from general and canonical representations of its surface topography. *Journal of the Optical Society of America. A, Optics, image science, and vision* **2006**, *23*, 219-232, doi:10.1364/josaa.23.000219.

7. Gómez, C.; Piñero, D.P.; Paredes, M.; Alió, J.L.; Cavas, F. Iterative Methods for the Biomechanical Evaluation of Corneal Response. A Case Study in the Measurement Phase. **2021**, *11*, 10819.

8. Ariza-Gracia, M.; Ortillés, Á.; Cristóbal, J.; Rodríguez Matas, J.F.; Calvo, B. A numerical-experimental protocol to characterize corneal tissue with an application to predict astigmatic keratotomy surgery. *Journal of the mechanical behavior of biomedical materials* **2017**, *74*, 304-314, doi:10.1016/j.jmbbm.2017.06.017.

9. Ariza-Gracia, M.; Zurita, J.; Piñero, D.P.; Calvo, B.; Rodríguez-Matas, J.F. Automatized Patient-Specific Methodology for Numerical Determination of Biomechanical Corneal Response. *Annals of biomedical engineering* **2016**, *44*, 1753-1772, doi:10.1007/s10439-015-1426-0.

10. Pandolfi, A. Cornea modelling. *Eye and vision (London, England)* **2020**, *7*, 2, doi:10.1186/s40662-019-0166-x.

11. Pandolfi, A.; Holzapfel, G.A. Three-dimensional modeling and computational analysis of the human cornea considering distributed collagen fibril orientations. *Journal of biomechanical engineering* **2008**, *130*, 061006, doi:10.1115/1.2982251.

12. Elsheikh, A.; Whitford, C.; Hamarashid, R.; Kassem, W.; Joda, A.; Büchler, P. Stress free configuration of the human eye. *Medical engineering & physics* **2013**, *35*, 211-216, doi:10.1016/j.medengphy.2012.09.006.

13. Lanchares, E.; Calvo, B.; Cristóbal, J.A.; Doblaré, M. Finite element simulation of arcuates for astigmatism correction. *Journal of biomechanics* **2008**, *41*, 797-805, doi:10.1016/j.jbiomech.2007.11.010.

14. Alastrué, V.; Calvo, B.; Peña, E.; Doblaré, M. Biomechanical modeling of refractive corneal surgery. *Journal of biomechanical engineering* **2006**, *128*, 150-160, doi:10.1115/1.2132368.

15. Alifa, R.; Piñero, D.; Velázquez, J.; Alió Del Barrio, J.L.; Cavas, F.; Alió, J.L. Changes in the 3D Corneal Structure and Morphogeometric Properties in Keratoconus after Corneal Collagen Crosslinking. *Diagnostics (Basel, Switzerland)* **2020**, *10*, doi:10.3390/diagnostics10060397.

16. Toprak, I.; Cavas, F.; Velázquez, J.S.; Alió Del Barrio, J.L.; Alió, J.L. Three-Dimensional Morphogeometric and Volumetric Characterization of Cornea in Pediatric Patients With Early Keratoconus. *American journal of ophthalmology* **2021**, *222*, 102-111, doi:10.1016/j.ajo.2020.09.031.

17. Elsheikh, A.; Wang, D.; Kotecha, A.; Brown, M.; Garway-Heath, D. Evaluation of Goldmann applanation tonometry using a nonlinear finite element ocular model. *Annals of biomedical engineering* **2006**, *34*, 1628-1640, doi:10.1007/s10439-006-9191-8.

18. Navarro, R.; Palos, F.; Lanchares, E.; Calvo, B.; Cristóbal, J.A. Lower- and higher-order aberrations predicted by an optomechanical model of arcuate keratotomy for astigmatism. *Journal of cataract and refractive surgery* **2009**, *35*, 158-165, doi:10.1016/j.jcrs.2008.09.015.

19. Pandolfi, A.; Manganiello, F. A model for the human cornea. Constitutive behavior and numerical analysis. *Biomechanics and Modeling in Mechanobiology* **2006**, *5*, 237-246. doi:10.1007/s10237-005-0014-x.

20. Gómez, F.S.; Lorza, R.L.; Bobadilla, M.C.; García, R.E. Improving the Process of Adjusting the Parameters of Finite Element Models of Healthy Human Intervertebral Discs by the Multi-Response Surface Method. *Materials (Basel, Switzerland)* **2017**, *10*, doi:10.3390/ma10101116.

Publicaciones DYNA SL  --  c) Mazarredo nº69 - 2º  -- 48009-BILBAO (SPAIN)
Tel +34 944 237 566 – www.revistadyna.com - email: dyna@revistadyna.com
Pag. 8 / 9

21. McCartney, W.; MacDonald, B.; Ober, C.A.; Lostado-Lorza, R.; Gómez, F.S. Pelvic modelling and the comparison between plate position for double pelvic osteotomy using artificial cancellous bone and finite element analysis. *BMC veterinary research* **2018**, *14*, 100, doi:10.1186/s12917-018-1416-1.

22. Somovilla-Gómez, F.; Lostado-Lorza, R.; Corral-Bobadilla, M.; Escribano-García, R. Improvement in determining the risk of damage to the human lumbar functional spinal unit considering age, height, weight and sex using a combination of FEM and RSM. *Biomechanics and modeling in mechanobiology* **2020**, *19*, 351-387, doi:10.1007/s10237-019-01215-4.

23. Chaudhry, H.R.; Bukiet, B.; Davis, A.; Ritter, A.B.; Findley, T. Residual stresses in oscillating thoracic arteries reduce circumferential stresses and stress gradients. *Journal of biomechanics* **1997**, *30*, 57-62, doi:10.1016/s0021-9290(97)81292-4.

24. Fung, Y.C. *Biomechanics: Mechanical Properties of Living Tissues*; Springer New York: 2013.

Publicaciones DYNA SL -- c) Mazarredo nº69 - 2º -- 48009-BILBAO (SPAIN)
Tel +34 944 237 566 – www.revistadyna.com - email: dyna@revistadyna.com

Pag. 9 / 9

ISSN: 0012-7361 eISSN: 1989-1490 / DYNA Vol.98 n.1 DOI: https://doi.org/10.6036/10649